water

MDPI

Article

Reduction of Cr(VI) by Synergistic Effects of Iron-Rich Biochar and *Pseudomonas aeruginosa*

Bei Ou †, Hui Wang †, Keke Xiao *, Yuwei Zhu, Yuan Liu, Sha Liang, Huijie Hou, Wenbo Yu, Jingping Hu and Jiakuan Yang

School of Environmental Science and Engineering, Huazhong University of Science and Technology, 1037 Luoyu Road, Wuhan 430074, China

* Correspondence: xiaokeke@hust.edu.cn; Tel.: +86-27-87540995

† These authors contributed equally to this manuscript.

Abstract: In view of the poisonous nature of Cr(VI), it is of great significance to explore an effective and environmentally friendly method to remove Cr(VI). The potential synergistic effects of Cr(VI) reduction by iron-rich biochar and *Pseudomonas aeruginosa* (PA) were systematically explored in this study. Significantly, in association with PA, the biochar produced by pyrolyzing iron-rich sludge at 300 °C (Fe-300) was more efficient at reducing Cr(VI) than that pyrolyzed at 800 °C (Fe-800), and the performance was always better than biochar or PA alone. For instance, upon an incubation for 20 days, the Cr(VI) removal efficiencies in the groups Cr + Fe-300 + PA, Cr + Fe-800 + PA, Cr + Fe-300, Cr + Fe-800 and Cr + PA were 80%, 19%, 51%, 0% and 35%, respectively. Through further analyses of phosphorus (P) and iron species as well as the cell extraction components of PA, the high Cr(VI) efficiency in Fe-300 + PA was mainly attributed to two aspects: (1) more P (mainly in the form of ortho phosphorus) was released from Fe-300 by PA compared to that from Fe-800, and the released P may react with Fe(II), Fe(III), Cr(VI) and Cr(III) ions to form precipitation; (2) cytoplasmic and periplasmic proteins as well as membrane proteins extracted from PA further helped to reduce Cr(VI). A novel approach for reducing Cr(VI) may be proposed by using the potential synergistic effects of iron-rich biochar and PA from this study.

Keywords: iron-rich sludge; biochar; *Pseudomonas aeruginosa*; chromium reduction; precipitation

Citation: Ou, B.; Wang, H.; Xiao, K.; Zhu, Y.; Liu, Y.; Liang, S.; Hou, H.; Yu, W.; Hu, J.; Yang, J. Reduction of Cr(VI) by Synergistic Effects of Iron-Rich Biochar and *Pseudomonas aeruginosa*. *Water* **2023**, *15*, 1159. https://doi.org/10.3390/w15061159

Academic Editor: Laura Bulgariu

Received: 13 February 2023
Revised: 11 March 2023
Accepted: 13 March 2023
Published: 16 March 2023

1. Introduction

Chromium is not only a ubiquitous environmental pollutant, but also damages human health and the growth of animals and plants [1,2]. Cr(III), a trace element closely related to the human body, is responsible for the human metabolism. However, Cr(VI), one of the most poisonous metals, shows carcinogenic and gene mutation-inducing effects. Cr(VI) is freely soluble in water, with toxicity as high as 100–1000 times that of Cr(III) [3,4]. Furthermore, various diseases have been linked to long-term exposure to Cr(VI) [5]. The leather, electroplating, printing, dyeing and metallurgy industries are the major sources of Cr(VI) [6]. The direct discharge of chromium-containing wastewater without any further treatment pollutes the ecosystem [7,8]. Consequently, more low-cost and specified methods should be investigated to reduce Cr(VI) to Cr(III) since conventional methods are either related to high expense or the use of chemical precipitants.

Currently, the proposed methods for Cr(VI) remediation include physical, chemical and biological methods [9–12]. Recently, sludge-based biochar has been widely used to alleviate Cr(VI) contamination by both physical adsorption and chemical reduction, with a superiority in adsorption properties, low cost and widely available sources [13,14]. Chen et al. found that the adsorption capacity of biochar towards Cr(III) was twice as high as that of Cr(VI) [15]. To enhance the efficiency of sludge-based biochar, Diao et al. firstly pyrolyzed biochar from sludge, and then immobilized nano zero valent iron on its surface

to obtain a new adsorbent towards adsorbing and reducing Cr(VI) [16]. However, in this case, extra zero valent iron was needed. The iron-rich sludge, produced from sludge dewatering typically with Fenton's reagents, was regarded as a promising source of iron by taking advantage of the indigenous iron present in waste sludge. The iron-rich sludge can be converted into a multifunctional biochar through pyrolysis to achieve resource recovery from sludge [17]. Pyrolysis temperatures increased substantially, causing the iron species to change significantly, which were namely from a high valent state to a low valent state, and finally even a zero valent state: $Fe_2O_3 \rightarrow Fe_3O_4 \rightarrow FeO \rightarrow Fe(0)$ [18,19]. Meanwhile, some studies showed that the pyrolysis temperature of biochar could affect Cr(VI) removal [20–22]. Despite this, the influence of iron-rich biochar in reducing Cr(VI) was not clearly identified, particularly at different pyrolysis temperatures when the species of indigenous iron in the iron-rich sludge changed accordingly. Therefore, a further investigation of the changes and mechanisms of biochar at different pyrolysis temperatures involved in Cr(VI) removal could provide a new method for efficient Cr(VI) treatment.

Besides biochar, bioremediation has also been widely used to detoxify Cr(VI). As one of multitudinous strains that can reduce Cr(VI), many studies have confirmed that *Pseudomonas* has a strong Cr(VI) reduction capability since chromium reductases were present in intracellular and extracellular cell membranes [23,24]. Sathishkumar et al. found that *Pseudomonas stutzeri* L1 showed the capability to reduce 97.0% of Cr(VI) at pH 8 and a temperature of 37 °C [25]. It was discovered that when the concentration of *Pseudomonas aeruginosa* (PA) rose from 0.5% (volume/volume, v/v) to 5% (v/v), the bioreduction of Cr(VI) increased from 46% to 83% at the initial Cr(VI) concentration of 20 mg/L upon an incubation for 12 h [26]. Cr(VI) was reduced efficiently with the carboxyl and amino functional groups in the cell wall of PA [27]. The enzymes secreted by PA, such as chromate reductases, were identified as the driving force for reducing Cr(VI) to Cr(III) through acting as cellular single-electron reductants [28]. However, currently most studies focus on the individual effects of either biochar or PA for reducing Cr(VI) and the potential synergistic effects of iron-rich biochar and PA remain unclear, particularly when the iron species on the iron-rich biochar vary, which presumably markedly improves the reduction efficiencies of Cr(VI). Previous studies have shown that PA, a representative phosphate solubilizing microorganism (PSM), is crucial in solubilizing phosphorus (P) in biochar [29]. Phosphate solubilizing microorganisms may promote the release of phosphorus on biochar in the aqueous phase, which could possibly form precipitation with co-existing chromium, phosphate and iron ions; however, this assumption also needs to be testified.

This study was intended to: (1) probe the potential synergistic effects of iron-rich biochar and PA on the reduction efficiency of Cr(VI) through testing variations in total chromium, Cr(VI) and Cr(III) concentrations; (2) investigate the reduction mechanism of Cr(VI) to Cr(III) through testing the protein extracts from different cell fractions, the changes in both the concentration and species of phosphorus and iron and investigating the possible precipitation of chromium, phosphate and iron ions. Detailed schematics are provided in Figure S1 (Supporting Information). Collectively, the results gained from this study may propose a novel method for reducing Cr(VI) by using the potential synergistic effects of iron-rich biochar and PA.

2. Materials and Methods

2.1. Iron-Rich Biochar Preparation

Raw sludge was taken from the concentration tank in a local wastewater treatment plant in Wuhan, China and its physicochemical characteristics were analyzed (Table S1, Supplementary Materials). A detailed description of biochar preparation is given in Text S1 of Supplementary Materials [30]. In brief, Fenton's reagents were firstly used in the raw sludge conditioning and then the sludge was dewatered [30]. After drying and sieving, pyrolysis was carried out at temperatures of 300 and 800 °C for the iron-rich sludge samples, which were labeled as Fe-300 biochar and Fe-800 biochar, respectively. In the preliminary study, the pyrolysis temperatures at 300, 500, 700, 800 and 900 °C were all tested for biochar

synthesis. From the results present in the previous studies [17], the biochar characteristics at the relatively low temperature of 300 °C and the relatively high temperature of 800 °C showed a significant difference in terms of iron species. Therefore, in this study, two representative temperatures of 300 °C and 800 °C were chosen.

2.2. The Cultivation of PA

Pseudomonas aeruginosa (CCTCC AB91095) was obtained from China Center for Type Culture Collection (CCTCC) (Hubei, China). Since the optical density of the strain in the logarithmic phase was between 0.8 and 2.0, the optimum cultivation time was chosen as 12 h according to its growth curve in Luria-Bertani medium (Figure S2, Supplementary Materials).

The medium used in the experiment contained Luria-Bertani medium and mineral liquid medium [31]. The former was normally used to activate bacteria, while the latter was used to prepare the incubation solution. The detailed compositions of Luria-Bertani medium and mineral liquid medium are provided in Table S2 (Supplementary Materials).

Activated PA, 0.8 mL, was dosed into a conical flask filled with 20 mL of Luria-Bertani medium and then the mixture was placed in a constant temperature incubator (37 °C, 150 revolutions per minute (rpm)) until the optical density was steady at 0.8–1. The residual bacterial pellets were obtained through centrifuging the cultivated bacterial suspension (6000 rpm, 10 min). After rinsing twice with mineral liquid medium, the bacterial pellets were collected, followed by adding 20 mL of inorganic salt medium and mixing thoroughly to prepare a bacterial suspension.

2.3. Experimental Procedures for the Reduction of Cr(VI) to Cr(III)

To investigate the individual and the potential synergistic effects of iron-rich biochar (Fe-300 and Fe-800) and PA on reducing Cr(VI), different experimental groups were set (Table 1). Taking into account the results of Qian et al., the doses of biochar (1 g/L) and PA (2%, *v*/*v*) were chosen [31]. Moreover, the choice of the dose of Cr(VI) (10 mg/L) was based upon the preliminary results that this concentration had no obvious effect on the growth of PA within 12 h [26] (Figure S3 in Supporting Information).

Table 1. The experimental design for the potential synergistic effects of iron-rich biochar and PA.

Experimental Objectives	Test Groups	Cr(VI) (mg/L)	Fe-300 (g/L)	Fe-800 (g/L)	Fe(II) (g/L)	Fe(0) (g/L)	PA (%, *v*/*v*)	The Determination Parameters
Section 2.3. Reduction of Cr(VI) to Cr(III) by Iron-Rich Biochar and PA	Cr (control group 1)	10	-	-	-	-	-	Cr
	Cr + PA	10	-	-	-	-	2	
	Cr + Fe-300	10	1	-	-	-	-	
	Cr + Fe-800	10	-	1	-	-	-	
	Cr + Fe-300 + PA	10	1	-	-	-	2	
	Cr + Fe-800 + PA	10	-	1	-	-	2	
Section 2.4.2. Phosphorus Release from Biochar by PA	Fe-300 (control group 2)	-	1	-	-	-	-	P
	Fe-800 (control group 3)	-	-	1	-	-	-	
	Cr + Fe-300	10	1	-	-	-	-	
	Cr + Fe-800	10	-	1	-	-	-	
	Fe-300 + PA	-	1	-	-	-	2	
	Fe-800 + PA	-	-	1	-	-	2	
	Cr + Fe-300 + PA	10	1	-	-	-	2	
	Cr + Fe-800 + PA	10	-	1	-	-	2	
Section 2.4.3. The Impacts of Different Iron Species on the Reduction of Cr(VI) to Cr(III)	Cr + Fe-300	10	1	-	-	-	-	Fe
	Cr + Fe(II)	10	-	-	1	-	-	
	Cr + Fe-800	10	-	1	-	-	-	
	Cr + Fe(0)	10	-	-	-	1	-	
	Cr + Fe-300 + PA	10	1	-	-	-	2	
	Cr + Fe(II) + PA	10	-	-	1	-	2	
	Cr + Fe-800 + PA	10	-	1	-	-	2	
	Cr + Fe(0) + PA	10	-	-	-	1	2	

Note: "-" means that nothing was added to the mixture.

Conical flasks of 250 mL were filled with the mineral liquid medium, Cr(VI), iron-rich biochar and PA, covered with vented sealing film (pore size of 0.22 μm) and then shaken at 150 rpm and 37 ± 1 °C. The total volume was 100 mL in each test. Besides, an experimental control group with only the addition of Cr(VI) solution (control group 1) or with only the addition of biochar samples (either Fe-300 biochar (control group 2) or Fe-800 biochar (control group 3)) was set up for comparison. Considering the main focus of this study was on reducing Cr(VI), instead of the phosphorus solubilization from biochar samples (which has previously been discussed throughout [17]), the experimental groups of PA, Fe-300 + PA and Fe-800 + PA were not investigated in this section. A longer incubation time beyond 20 days may further improve the Cr(VI) removal efficiency. However, to maintain a neutral pH of the incubation solution, an incubation time of 20 days was set herein. The aqueous phase of the mixture was determined for total chromium, Cr(VI) and Cr(III) concentrations on the 0th, 1st, 2nd, 5th, 7th, 10th, 15th and 20th day. The concentration of total chromium in the solid phase was investigated on the 20th day as well. The Cr(VI) reduction efficiency was calculated from Equation (1).

$$\text{The Cr(VI) reduction efficiency} = (C_0 - C_t)/C_0 \times 100\% \quad (1)$$

Noted: C_0 means Cr(VI) concentration on the 0th day;
C_t means Cr(VI) concentration on the tth day.

2.4. The Different Processes of the Potential Synergistic Reduction of Cr(VI) by Iron-Rich Biochar and PA

2.4.1. Preparations of Cell Components and Chromium Reductase Activity Assays

To extract different cell components of bacteria (cytoplasmic and periplasmic proteins and cell membrane proteins), 1× phosphate buffered saline (PBS) was used. Following the methods described in Zhang et al. [32], PA was cultivated in Luria-Bertani medium for 12 h. The supernatant after centrifugation was discarded by rinsing the bacteria twice with PBS. The washed bacteria were added into the inorganic salt medium by shaking at 35 °C for 24 h. A resuspension of the collected strain was performed in the PBS buffer before sonicating in an ice water bath for 30 min. The crude cell extract in the supernatant was obtained by high-speed centrifugation (10,000× *g*, 5 min). Afterwards, the supernatant was further centrifuged (150,000× *g*, 2 h) and labeled as cytoplasmic and periplasmic proteins, and the pellet was resuspended in PBS as cell membrane protein. To reduce Cr(VI), 1 mL of the reaction mixture contained 0.1 mL of protein extracts, 0.1 mM of nicotinamide adenine dinucleotide solution and 1 mg/L of Cr (VI) and then was incubated at 35 °C for 30 min. Upon completing the incubation, a determination of Cr(VI) remaining concentration was conducted.

2.4.2. The Changes of Phosphorus Concentration and Species

To investigate the reduction mechanism of Cr(VI), the total phosphorus (TP) concentration and different phosphorus species solubilized from biochar in the aqueous phase (Fe-300, Fe-800, Cr + Fe-300, Cr + Fe-800, Fe-300 + PA, Fe-800 + PA, Cr + Fe-300 + PA and Cr + Fe-800 + PA) were monitored on the 0th, 1st, 2nd, 5th, 7th, 10th, 15th and 20th day. Phosphorus species of biochar in the solid phase (Fe-300, Fe-800, Fe-300 + PA, Fe-800 + PA, Cr + Fe-300, Cr + Fe-800, Cr + Fe-300 + PA and Cr + Fe-800 + PA) were also tested on the 20th day. Phosphorus species in the aqueous and solid phases are shown in Table S3 (Supplementary Materials).

2.4.3. The Impacts of Different Iron Species on the Reduction of Cr(VI) to Cr(III)

Pure substances (Fe(II) in the form of $FeSO_4 \cdot 7H_2O$ and Fe(0) in the form of zero valent iron) were adopted to investigate iron reduction on biochar surface with the same dose of biochar (1 g/L). The detailed doses in the groups Cr + Fe-300, Cr + Fe(II), Cr + Fe-800, Cr + Fe(0), Cr + Fe-300 + PA, Cr + Fe(II) + PA, Cr + Fe-800 + PA and Cr + Fe(0) + PA are

shown in Table 1. The iron concentrations (total iron, Fe(II) as well as Fe(III)) in the aqueous phase were determined after 30 min.

2.5. Analytical Methods

The analyses for chromium concentration (total chromium, Cr(VI) and Cr(III)), interaction effects (E), phosphorus (total phosphorus and different species both in the aqueous and solid phase), iron and the binding states of iron by X-ray photoelectron spectroscopy (XPS) are described in Text S2 of Supplementary Materials.

The microscopic morphology of samples was performed using Nova Nano SEM 450 field emission scanning electron microscope produced by FEI Company in the Netherlands. Signal acquisition was performed on the target area of samples with energy-dispersive spectroscopy (EDS).

2.6. Statistical Analysis

Triplicates were conducted for each test. The comparisons among different groups were applied with least-significant difference (LSD) for one-way analysis of variance (ANOVA) at a significance level of 0.05 ($p < 0.05$). The results were also applied with t-test to perform statistical analysis by SPSS Statistics 18.0 (International Business Machines Corporation, Armonk, NY, USA). The error bars of all figures represent the standard deviation (SD).

3. Results and Discussion

3.1. Reduction of Cr (VI) to Cr(III) by Iron-Rich Biochar and PA

3.1.1. Changes of Total Chromium Concentration

During the 20 days' incubation, changes of approximately 0%, 8%, 1% and 10% in the groups Cr, Cr + PA, Cr + Fe-800 and Cr + Fe-800 + PA, respectively, could be observed in the total chromium concentrations in the aqueous phase (Figure 1a,b,d,f). Total chromium concentrations remained almost unchanged in the aqueous phase, indicating that there might be soluble organo-Cr(III) complexes that would not precipitate [33,34]. However, the decreased concentrations of total chromium in the groups Cr + Fe-300 and Cr + Fe-300 + PA (9.1 to 6.2 mg/L and 9.1 to 4.3 mg/L) with time lapsing in the aqueous phase were clearly noted (Figure 1c,e), which was possible because the reduced Cr(III) precipitated on biochar [35].

To further confirm the above assumption, solid samples in 100 mL of the reaction mixture were collected for the analysis of total chromium concentration (Figure 2). The chromium in the biochar was almost unchanged in Cr + Fe-800 and Cr + Fe-800 + PA for 0.0325 mg and 0.0307 mg compared to the initial Fe-300 biochar (0.0237 mg) and Fe-800 biochar (0.0291 mg). In the solid phase of the groups Cr + Fe-300 and Cr + Fe-300 + PA, an obvious increase in chromium concentration was noted and about 0.0885 mg and 0.1347 mg of chromium shifted from the aqueous phase to the solid phase (Figure 2). Cr(VI) appeared to be reduced in the solid phase as well, which further proved the speculation surrounding precipitation in Fe-300 biochar with or without the presence of PA. The lost part may be due to the long-term shaking of the culture and repeated sampling (Figure 2).

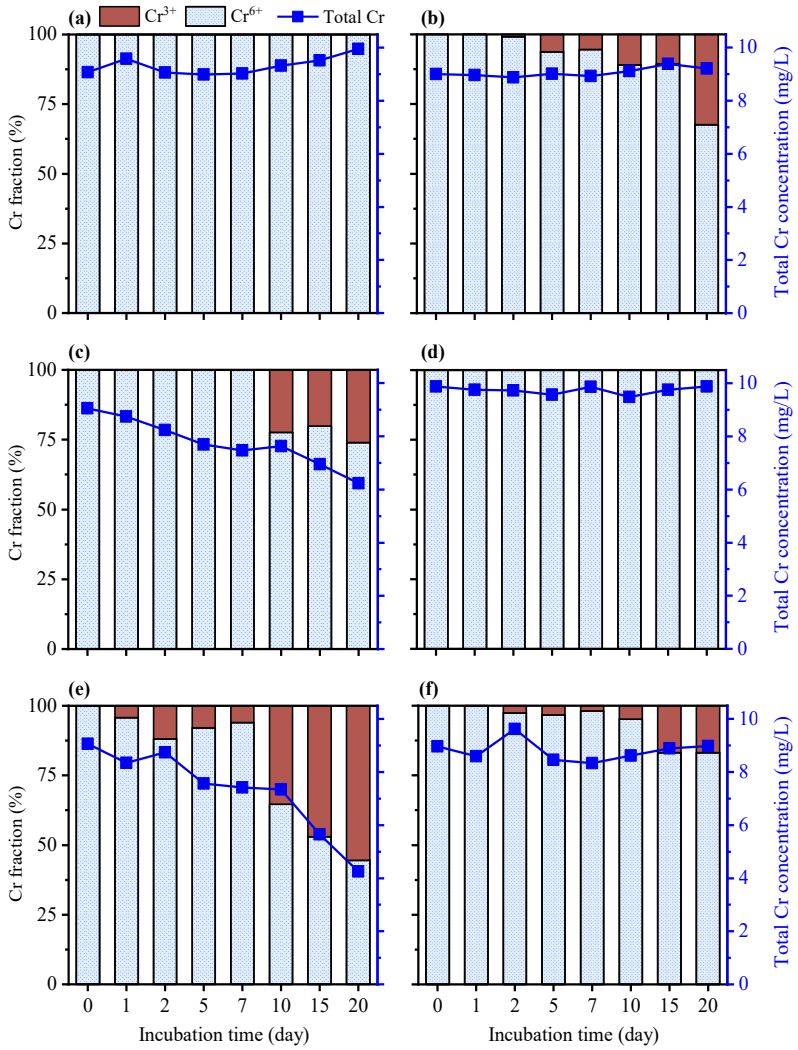

Figure 1. Total chromium, Cr(VI) and Cr(III) concentrations in different experimental groups during 20 days' incubation: (**a**) Cr, (**b**) Cr + PA, (**c**) Cr + Fe-300, (**d**) Cr + Fe-800, (**e**) Cr + Fe-300 + PA and (**f**) Cr + Fe-800 + PA.

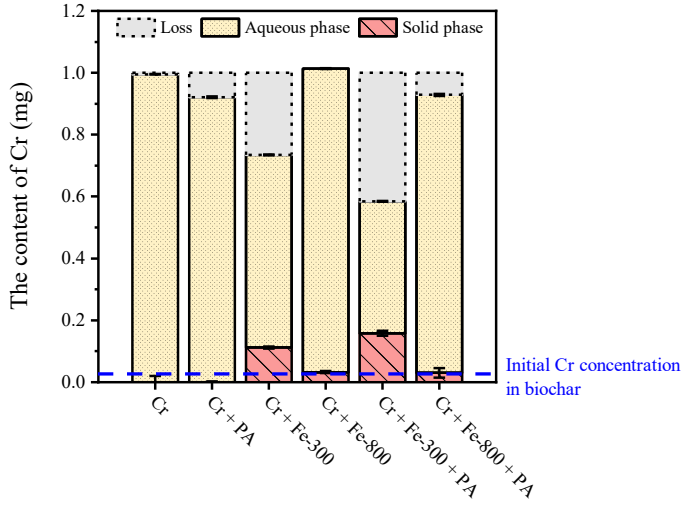

Figure 2. The mass balance of chromium (total volume of 100 mL). Noted: "Loss" means the loss of chromium compared to initial total chromium.

3.1.2. The Changes of Cr(VI) and Cr(III)

The concentration of Cr(VI) in Cr (control group 1) without adding iron-rich biochar and PA basically did not change since no reduction reaction occurred (Figure 1a). Comparing the experimental groups of Cr and Cr + PA, even when the total chromium concentration remained the same, the percentage of Cr(VI) in Cr + PA began to show a downward trend on the 2nd day, namely from 9.6 mg/L to 6.3 mg/L, revealing that Cr(VI) might be reduced to Cr(III) by PA. The results of Zhou and Chen supported the finding that, when the initial concentration of Cr (VI) was 1.2 mg/L, the *Pseudomonas* sp. strain JF122 could completely reduce Cr (VI) within 72 h [36]. Upon the completion of incubation for Cr + PA, the Cr(VI) and Cr(III) concentrations (6.2 and 3.0 mg/L, respectively) accounted for 68% and 32% of the total chromium, respectively (Figure 1b).

As for the Cr(VI) concentrations in the groups Cr (9.9 mg/L), Cr + Fe-800 (10.0 mg/L) and Cr + Fe-800 + PA (7.5 mg/L) on the 20th day, Cr + Fe-800 + PA showed the maximum Cr(VI) reduction effect of 25%, which could be the enzymatic reaction of PA or the reduction of iron on the Fe-800 biochar surface [37], and this is discussed in more detail in the subsequent section. However, as PA was absent, since the variation of Cr valence remained unchanged in Cr + Fe-800 within 20 days (Figure 1a,d,f), it was speculated that PA may have a stronger effect on Cr(VI) reduction than iron on the Fe-800 biochar surface. Similarly to the group Cr + PA, Cr(VI) started to be reduced in the group Cr + Fe-800 + PA on the 2nd day as Cr(III) concentration gradually rose to 1.5 from 0 mg/L. The reduced efficiency in the combination of Fe-800 and PA may be due to the fact that the corrosion of Fe^0 produces OH^- (Equation (2)), which raises the pH value in the reaction system beyond the optimum survival range of PA, thus resulting in the worse removal efficiency of Cr(VI).

$$Fe^0 + 2H_2O \rightarrow Fe^{2+} + 2OH^- + H_2 \quad (2)$$

In comparison to Cr (control group 1), the Cr(VI) concentrations in the groups Cr + Fe-300 and Cr + Fe-300 + PA trended downwards within the incubation time, namely from the 0th day (9.4 mg/L, 100% of the total chromium in Cr + Fe-300 and 9.5 mg/L, 100% of the total chromium in Cr + Fe-300 + PA) to the 20th day (4.6 mg/L, 74% of the total chromium in Cr + Fe-300 and 1.9 mg/L, 45% of the total chromium in Cr + Fe-300 + PA) (Figure 1a,c,e). Cr(VI) in Cr + Fe-300 was reduced on the 10th day with the Fe-300 biochar present, indicating that Fe-300 biochar was capable of reducing Cr(VI), and Zhang et al. [38] also noticed the Cr(VI) reduction extent by pristine biochar at the 200th h. Furthermore, the Cr(III) concentrations in Cr + Fe-300 + PA began to increase on the 1st day with the addition of PA, indicating the potential synergistic reduction by Fe-300 biochar and PA. After incubation, the Cr(VI) reduction efficiency (80%) in the group Cr + Fe-300 + PA was better than that in the group Cr + Fe-300 (51%) given the enzymatic reaction and the possible precipitation of chromium, phosphate and iron ions, which are discussed later.

In contrast, the Cr(VI) concentrations in the groups Cr + Fe-800 and Cr + Fe-300 were reduced from 10 and 9.4 mg/L initially to 9.9 (100% of the total chromium) and 4.6 mg/L (74% of the total chromium) on the 20th day, respectively. Accordingly, Cr + Fe-300 achieved the optimal Cr(VI) reduction of 51% at the 20th day (Figure 1c,d). In the groups Cr + Fe-800 + PA and Cr + Fe-300 + PA, there was a greater reduction effect on Cr(VI) for the former than the latter, which may be related to the different iron species in Fe-800 and Fe-300 biochars. As for the interaction effects of PA and biochar (Figure S4, Supporting Information), the values of E in the group Cr + Fe-800 + PA changed greatly and were positive ($E > 0$) only on the 2nd and 15th days. At the beginning of the process in the group Cr + Fe-800 + PA, possibly due to the strong adaptability and rapid growth of PA, the ability to reduce the Cr(VI) of PA was much stronger, resulting in a strong change in Cr(VI) reduction efficiency leading to a high value of interaction effects. On the other hand, there was small wave range in the values of E in the group Cr + Fe-300 + PA, which were all positive. It was indicated that PA and Fe-300 biochar exhibit an excellent synergistic effect on Cr(VI) reduction, consistent with the phenomenon in Figure 1.

It was observed that the Cr(VI) removal efficiency of biochar and microorganisms was lower than the results reported in some previous studies with the addition of lactic acid at the same reaction time (Table S4, Supporting Information). Apart from the reason for the acid condition in the original systems, lactic acid, a weak electron donor, could lead to a marked enhancement of Cr(VI) reduction at lower pH levels [39]. Since there were many different and complex reaction systems in the Cr(VI) reduction process (such as the preparation and dose of biochar, the initial Cr(VI) concentration, pH value, the amounts of inocula, the incubation time, etc.), the Cr(VI) reduction efficiency would obviously differ for every study.

3.2. Different Processes of Iron-Rich Biochar and PA Synergistic Reduction of Cr(VI)

3.2.1. The Cr(VI) Reduction Effect of Protein Extracts from Different Cellular Components

Pseudomonas aeruginosa was separated into cytoplasmic and periplasmic proteins as well as membrane proteins by centrifugation [32]. The percentages of reduced Cr(VI) by cytoplasmic and periplasmic proteins as well as membrane proteins were 64% and 78%, respectively (Figure S5, Supplementary Materials), showing that there might be some intracellular and membrane proteins in the bacterium that were capable of reducing Cr(VI). This is because the cytoplasmic, periplasmic and membrane proteins of bacteria possess some Cr(VI) reductase activities [40]. Additionally, it is obvious that membrane proteins have higher Cr(VI) reductase activity than cytoplasmic and periplasmic proteins.

3.2.2. Phosphorus Release from Biochar by PA

In the case of the change of total phosphorus for the aqueous phase, the TP concentrations of the four groups without Cr(VI) increased significantly with time, i.e., Fe-300 (from 0.08 to 1.26 mg/L), Fe-800 (from 0.12 to 1.98 mg/L), Fe-300 + PA (from 0.04 to 2.46 mg/L) and Fe-800 + PA (from 0.16 to 1.65 mg/L) (Figure 3a,b,e,f). This might be explained by water leaching a fraction of available phosphorus from biochar [41]. The results of the released TP were applied to the paired sample t-test to perform statistical analysis. During 20 days' incubation, compared with control groups, Fe-300 + PA was more effective in solubilizing phosphorus than Fe-300, while Fe-800 + PA showed little difference to Fe-800, which agreed with the previous research [29]. It is inferred that both Fe-300 and PA might provide more benefits for reducing Cr(VI). The concentrations of TP in the groups with Cr(VI) (e.g., Cr + Fe-300, Cr + Fe-800, Cr + Fe-300 + PA, Cr + Fe-800 + PA) were at a lower level of about 0.44–0.73 mg/L on the 20th day (Figure 3c,d,g,h). It is highly possible that a certain part of the phosphorus in the aqueous phase may react with Cr(III) or Cr(VI).

For those groups without the addition of PA, the species of phosphorus in the aqueous phase did not change significantly in the two control groups (Fe-800 and Fe-300), but the proportion of orthophosphate (ortho-P) in the groups with Cr(VI) gradually increased over time (e.g., 41% on the 1st day versus 81% on the 20th day in the group Cr + Fe-800, and 38% on the 1st day versus 89% on the 20th day in the group Cr + Fe-300), showing that there was a transformation of the released pyrophosphates from the biochar (pyro-P) to ortho-P (Figure 3a–d).

As for the groups with PSM, the proportion of phosphorus sorbed by PA (microbe-P) reached the maximum on the 5th or 7th day, showing the phosphorus-solubilizing effect of PA (e.g., 32% of total P in the group Fe-800 + PA, 54% of total P in Cr + Fe-800 + PA on the 7th day, 43% of total P in the group Cr + Fe-300 + PA on the 5th day and 34% of total P in Fe-300 + PA). Yu et al. found that the maximum phosphorus solubilization produced by the strain *Pseudomonas* sp. YLYLP29 occurred on the 6th day, which was consistent with the findings in this study [42]. The proportion of pyro-P gradually decreased and even disappeared (e.g., Cr + Fe-800 + PA and Cr + Fe-300 + PA on the 20th day) during the incubation process, which was presumed to be related to the transformation of ortho-P (Figure 3e–h), since PSM mainly transformed phosphorus from insoluble forms into monobasic and dibasic phosphate (HPO_4^{2-} and $H_2PO_4^-$) [29,43]. With the decrease in

pyro-P release and the conversion from pyro-P to ortho-P, Cr(III) or Cr(VI) is more likely to react with ortho-P and then to form various Cr-P precipitates [44].

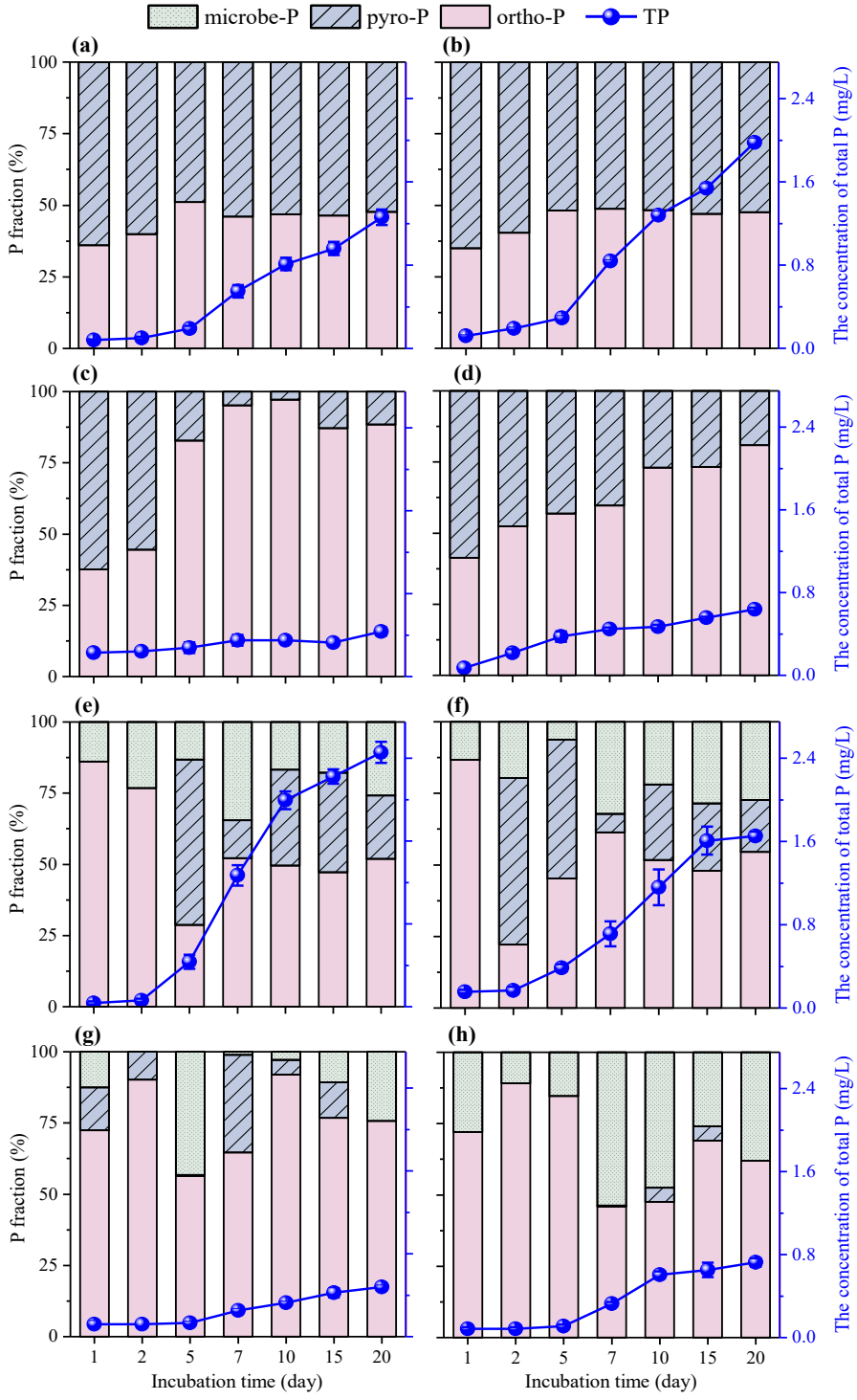

Figure 3. The concentrations of total P and different P species in the aqueous phase during 20 days' incubation: (**a**) Fe-300, (**b**) Fe-800, (**c**) Cr + Fe-300, (**d**) Cr + Fe-800, (**e**) Fe-300 + PA, (**f**) Fe-800 + PA, (**g**) Cr + Fe-300 + PA and (**h**) Cr + Fe-800 + PA.

Compared with the initial values of Fe-800 biochar (36.3 mg/g) and Fe-300 biochar (22.0 mg/g), the total phosphorus concentration of biochar decreased in all groups after 20 days' incubation. Concerning the four groups with Fe-800 biochar on the 20th day (Fe-800,

Cr + Fe-800, Fe-800 + PA and Cr + Fe-800 + PA), it can be seen that there was an indiscernible change in the total phosphorus concentration of biochar (21.9–23.0 mg/g). In regard to the groups with the addition of Fe-300 biochar, the decline sequence in the total phosphorus concentration of biochar was Fe-300 ≈ Cr + Fe-300 < Cr + Fe-300 + PA < Fe-300 + PA; the concentrations of total phosphorus on the 20th day were 19.9, 20.3, 17.0 and 14.4 mg/g, respectively. The total phosphorus concentration on biochar fell from 22.0 to 19.88 mg/g for Fe-300 and 14.38 mg/g for Fe-300 + PA, while the residual phosphorus concentration on biochar was Fe-300 + PA > Cr + Fe-300 + PA (14.38 mg/g and 17.00 mg/g) (Figure 4a), presumably because a certain part of the released phosphorus reacted with iron, Cr(III) or Cr(VI) to form iron, chromium and phosphorus precipitation [45,46].

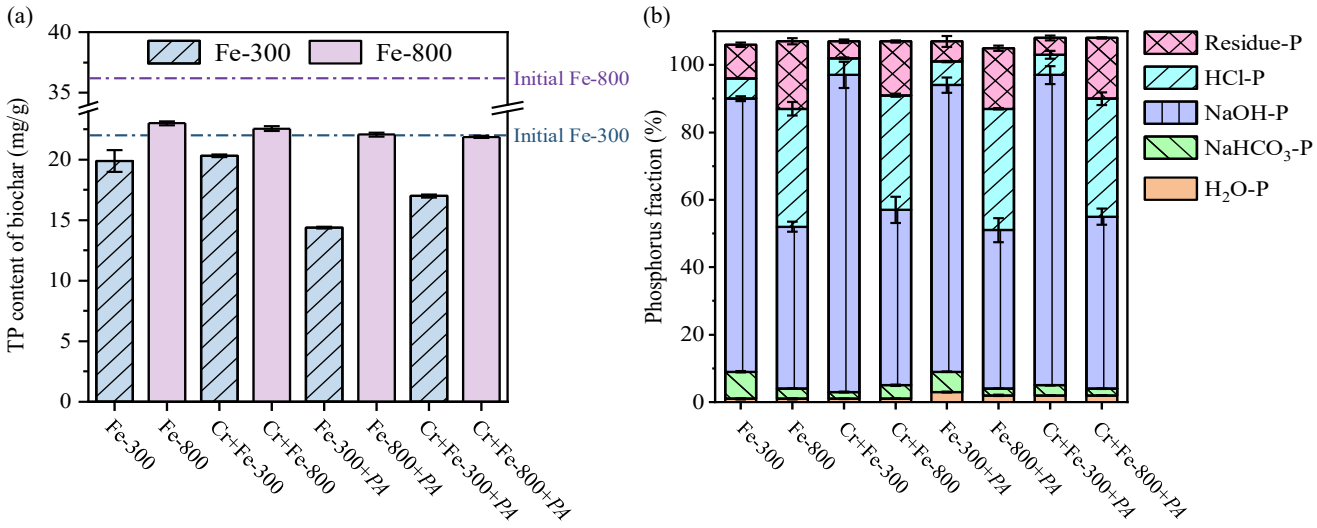

Figure 4. Changes in (**a**) total phosphorus concentration and (**b**) different phosphorus species on the 20th day.

With changes in five phosphorus species of biochar, phosphorus release from biochar by PA was investigated (Figure 4b). The summation of water-soluble phosphorus (H_2O-P) and exchangeable phosphorus ($NaHCO_3$-P) in Fe-800 biochar was lower than in Fe-300 biochar, revealing that Fe-300 biochar contained more bio-available phosphorus than Fe-800 biochar [47]. Iron aluminum bound phosphorus (NaOH-P) in Fe-800 groups (Fe-800, Cr + Fe-800, Fe-800 + PA and Cr + Fe-800 + PA) accounted for 47–52%, taking up a majority of phosphorus species, and calcium magnesium bound phosphorus (HCl-P) and residual phosphorus (residual-P) occupied about 50–55% (Figure 4b). This was the same as the Fe-800 groups: NaOH-P in the Fe-300 groups (Fe-300, Cr + Fe-300, Fe-300 + PA and Cr + Fe-300 + PA) was the majority (accounting for around 85%), while HCl-P and residual-P represented only a fraction, about 13%. From the proportion of more steady state P (HCl-P and Residual-P), it is apparent that the phosphorus species in Fe-800 biochar were more stable than in Fe-300 biochar. The polymerization degree of phosphorus minerals on biochar prepared by low-temperature pyrolysis was relatively low, so the stability of Fe-300 biochar was lower than that of Fe-800 biochar [48,49]. Comparing the Fe-300 biochar group and the Fe-800 biochar group, there were unobservable changes of phosphorus species, showing that PA only increased the total concentration of solubilized phosphorous from biochar rather than affecting phosphorus species within the tested conditions in this experiment [31].

3.2.3. The Impacts of Different Iron Species on the Reduction of Cr(VI) to Cr(III)

As the pyrolysis temperature increased, part of the iron species shifted from Fe(II) and Fe(III) to Fe(0) in the Fe-800 biochar (Figure S6, Supporting Information). Various iron

species responsible for Cr(VI) reduction were investigated with pure substances (Fe(II), ions and Fe(0)) during 30 min incubation (Table 2). Differently from Fe(II), which was easily soluble in water, Fe-300 biochar, Fe-800 biochar and Fe(0) were nearly insoluble in water, so the initial iron concentrations in these groups were almost zero.

Table 2. The iron concentrations of experimental groups after incubation for 30 min (mg/L).

Test Groups	Fe(II)	Fe(III)	Total Fe
Cr + Fe-300	0.69	0.12	0.81
Cr + Fe(II)	302.61	4.81	307.42
Cr + Fe-800	0.21	0.49	0.70
Cr + Fe(0)	1.65	0.29	1.94
Cr + Fe-300 + PA	0.45	0.15	0.60
Cr + Fe(II) + PA	268.30	12.75	281.05
Cr + Fe-800 + PA	0.41	0.04	0.45
Cr + Fe(0) + PA	0.52	0.37	0.89

The concentrations of Fe(II) or Fe(III) were maintained at a low and almost constant level in the Fe(0)-dominated experimental groups without PA (e.g., 0.21 and 1.65 mg/L for Fe(II), 0.49 and 0.29 mg/L for Fe(III) in Cr + Fe-800 and Cr + Fe(0), respectively). Much past work has examined an acid environment facilitating Cr(VI) reduction to Cr(III) and increased iron dissolution in biochars with Fe(0) [50,51]. It is probably demonstrated that the Cr(VI) reduction effect of iron on Fe-800 biochar was weak at neutral pH, since the iron surface might be in a passive state, thus decreasing the quantity of Fe species reducing Cr(VI). Even the addition of PA insignificantly affected the concentrations of Fe(II) and Fe(III) in Cr + Fe-800 + PA (0.41 mg/L for Fe(II) and 0.04 mg/L for Fe(III)) and Cr + Fe(0) + PA (0.52 mg/L for Fe(II) and 0.37 mg/L for Fe(III)). The iron-rich biochar prepared by pyrolysis at 800 °C was mainly Fe(0), which had difficulty reacting with Cr(VI) in a neutral condition; hence, there was no accumulation of Cr(III).

Comparing the Fe-300 group with the Fe-800 group, Fe-300 biochar could dissolve partial Fe(II) and Fe(III) from its surface, which may be because Fe(II) and Fe(III) predominated in Fe-300 biochar. The Fe(II) concentration in Cr + Fe-300 was low (0.69 mg/L), since an interaction between Cr(VI) and Fe(II) dissolved from Fe-300 biochar might convert Cr(VI) to Cr(III) (Equation (3)), as indicated in the significant decrease for Fe(II) concentration. Similar phenomena were also observed by using Fe(II) pure substance: the Fe(II) concentrations of the groups Cr + Fe(II) and Cr + Fe(II) + PA decreased from the initial 1000 to 302.61 and 268.30 mg/L, respectively (Figure S7a, Supplementary Materials). This may be because of the reaction between Cr(VI) and Fe(II) resulting in Cr(III) and Fe(III) (Equation (3)). When Fe-300 biochar was present, Fe(III) could be removed from the aqueous phase by adsorbing Fe(III) onto Fe-300 biochar and precipitating $Fe(OH)_3$ [52]. Furthermore, the concentration of Fe(II) in Cr + Fe-300 + PA (0.45 mg/L) was as low as that in the group Cr + Fe-300, indicating that Cr(VI) could react with Fe(II), and the addition of PA had an unobservable influence on the iron concentration but showed a great influence on phosphorus concentration.

Overall, whether for Fe-800 biochar or Fe-300 biochar, the addition of PA did not affect iron concentration, but more affected phosphorus concentration as well as the secretion of Cr(VI) reductase. The results depicted in Figure S7b (Supplementary Materials) were the further proof of the different Cr(VI) reduction effects of Fe-800 and Fe-300 biochars. Fe-300 biochar with Fe(II)/Fe(III) on its surface had a higher tendency to undergo a reaction for reducing Cr(VI) at neutral pH, while iron on the surface of Fe-800 biochar barely reacted with Cr(VI). Besides, upon making contact with Fe-300 biochar, the generated Cr(III) combined with Fe(II)/Fe(III), allowing precipitation because of the depletion of protons as the reaction proceeded (Equations (4)–(6)) [53]. It is therefore deduced that both iron and the existence of redox-active metal played important roles in the biochar redox mediation properties [54]. The precipitation of Cr and Fe usually occurred at alkaline pH

values, OH^- and Cr(VI) anions would compete for adsorption sites and hydroxides would be deposited on the biochar surface, resulting in reduced Cr(VI) removal efficiency [55]. Besides, the precipitation could block the adsorption of Cr(VI) in the solution onto the pores or on the biochar surface [56]. Therefore, the precipitation of Cr and Fe may to some extent affect the adsorption efficiency of the biochar.

3.2.4. Morphology Characteristics of Biochar and PA

The individual morphology of PA was a short rod with a rough and uneven surface (Figure 5a). It has been observed that the spherical structure of iron oxides is gradually broken into smaller cubical fragments with the increase in pyrolysis temperature, indicating a phase transition of iron that could also be found in the Fe-300 and Fe-800 biochars (Figure 5b,c) [57]. Possibly due to the release of Fe(II) from Fe-300 biochar and its reaction with Cr(VI), the independently stacked flakes were linked into sheets, since Cr(VI) might co-precipitate with Fe(II) as well as Fe(III) on the biochar surface (Figure 5e) compared with the independently stacked flakes on the Fe-300 biochar surface (Figure 5b) [58]. The rod-shaped PA was present on the biochar surface, possibly due to the interaction of Fe-300 with PA (Figure 5d). As for Fe-800 biochar groups, the morphologies with rough surfaces and plenty of pores showed unobservable changes in the groups Fe-800, Fe-800 + PA and Cr + Fe-800 (Figure 5c,g,h). As a result of the potential reaction between PA, biochar (Fe-300 and Fe-800 biochar) and chromium (Figure 5d,g), the biochar and bacteria were closely linked considering the physical and chemical interactions. However, the shape and structure of bacteria were not noticeable in Cr + Fe-300 + PA, which might be due to the fact that Fe(II) on the biochar surface consumed H^+ during the redox reaction, accompanied with the increased pH of the entire reaction system (Equation (3)). While the respective pH values were alkaline at 8.71 and 8.61 in Cr + Fe-300 + PA and Cr + Fe-800 + PA on the 20th day, PA would suffer from autolysis [59], resulting in the inconspicuous morphology of PA.

$$6Fe^{2+} + Cr_2O_7{}^{2-} + 14H^+ \rightarrow 6Fe^{3+} + 2Cr^{3+} + 7H_2O \quad (3)$$

$$aFe^{3+} + bCr^{3+} + 3H_2O \rightarrow Cr_bFe_a(OH)3 + 3H^+ \quad (4)$$

$$aFe^{3+} + bCr^{3+} + 2H_2O \rightarrow Cr_bFe_aOOH + 3H^+ \quad (5)$$

$$2Cr^{3+} + Fe^{2+} + 4H_2O \rightarrow FeCr_2O_4 + 8H^+ \quad (6)$$

Noted: a + b = 1.

For the EDS analysis of PA, the P (mass percentage of 3.14%) may be derived from the cell wall, which possessed phosphoryl functional groups at the surface [60], while Fe and Cr were not detected (Figure S8a, Supplementary Materials). Fe-300 biochar groups with the obvious reduction on Cr(VI) were selected and characterized to further explore the mechanism of biochar and PA synergistic reduction. Fe (mass percentages of 16.40% and 18.19%) and P (mass percentages of 7.48% and 3.92%) were detected, respectively, in Fe-300 and Fe-300 + PA, but chromium was not found, probably because the chromium concentration on the biochar was below the detection limit (Figure S8b,c, Supplementary Materials). For the groups with Cr(VI), the mass percentages of Cr in Cr + Fe-300 (0.55%) and Cr + Fe-300 + PA (1.00%) increased obviously, which proved that the chromium originally in the aqueous phase was precipitated on the biochar by comparing the concentration of chromium between Fe-300 and Fe-300 + PA (Figure S8d,e, Supplementary Materials).

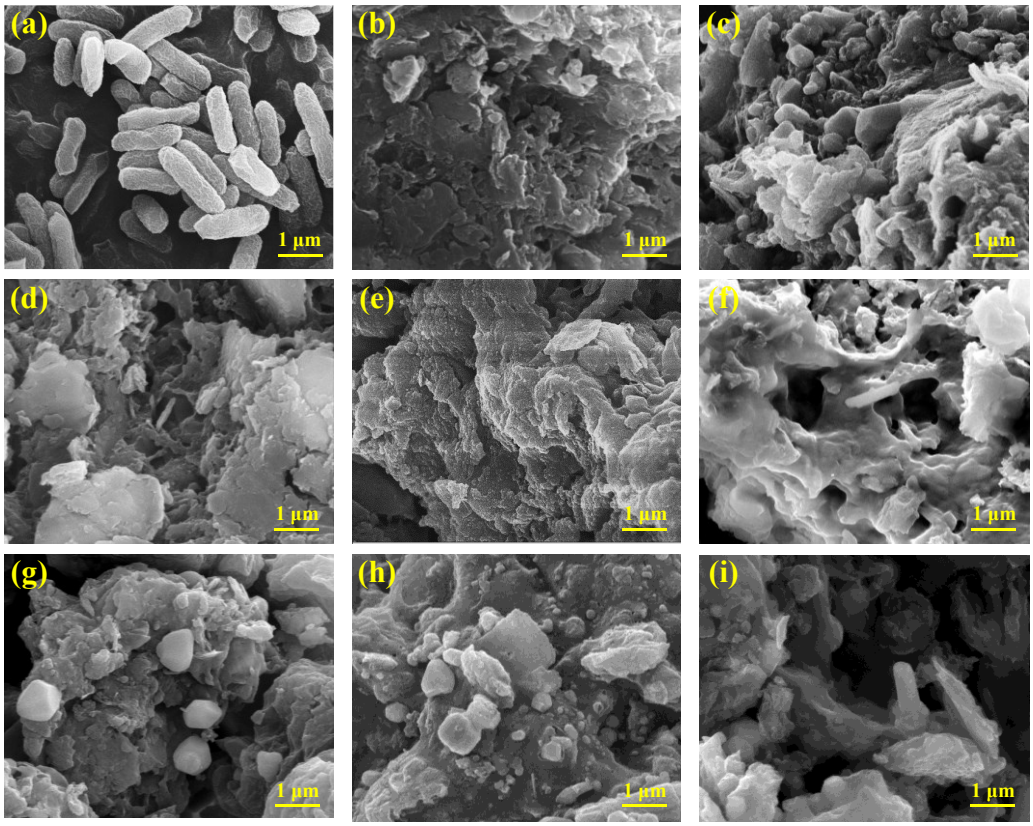

Figure 5. The SEM of (**a**) PA, (**b**) Fe-300, (**c**) Fe-800, (**d**) Fe-300 + PA, (**e**) Cr + Fe-300, (**f**) Cr + Fe-300 + PA, (**g**) Fe-800 + PA, (**h**) Cr + Fe-800 and (**i**) Cr + Fe-800 + PA.

4. Conclusions

This systematic study of the potential synergistic effects of Cr(VI) reduction by iron-rich biochar and PA was conducted herein. It was demonstrated that the reduction efficiency of Cr(VI) reached a maximum of 80% after 20 days' cultivation upon the combined effects of Fe-300 biochar and PA. The cytoplasmic and periplasmic proteins as well as membrane proteins extracted from PA were active with Cr(VI) reductase. The addition of PA promoted more P release from Fe-300 biochar than that from Fe-800 biochar, and the total phosphorus concentration of Fe-300 biochar decreased from 19.88 to 14.38 mg/g. However, the phosphorus concentration on Fe-800 biochar did not change significantly. Moreover, the released phosphate precipitated with Cr(VI) and Cr(III) on the biochar surface, reducing the total chromium concentration in the aqueous phase. Within neutral conditions, Fe-300 biochar alone was more efficient at Cr(VI) reduction than Fe-800 biochar due to the different predominant iron species present therein. Besides the bench-scale tests performed in this study, more scale-up studies are needed in future work to further indicate the synergistic effects of biochar and PA in Cr(VI) removal, while considering more complex factors such as the impacts of organic matter and minerals.

Supplementary Materials: The following supporting information can be downloaded at: https://www.mdpi.com/article/10.3390/w15061159/s1, Text S1: Iron-Based Biochar Preparation, Text S2: Testing and Characterization Methods; Table S1: Main characteristics of raw sludge, Table S2: Chemical composition of culture medium, Table S3: Phosphorus species in the aqueous and solid phase, Table S4: The comparison of the reduction of Cr(VI) with other studies; Figure S1: The schematic of this study, Figure S2: The growth curve of PA, Figure S3: Effect of Cr(VI) concentration on the growth of PA, Figure S4: Interaction effects of PA and biochar, Figure S5: The effect of protein extracts from various cellular components on reducing Cr(VI), Figure S6: Fe 2p XPS profiling spectra of (a) Fe-300 and (b) Fe-800 at the pyrolysis temperatures of 300 °C and

800 °C, respectively, Figure S7: (a) The picture shows the reaction of Cr(VI) and Fe(II) and (b) the changes of Cr(VI) concentration in Fe-300, Fe-800, Cr + Fe-300 and Cr + Fe-800 groups as the incubation process proceeded, Figure S8: The EDS of (a) PA, (b) Fe-300, (c) Fe-300 + PA, (d) Cr + Fe-300 and (e) Cr + Fe-300 + PA, Figure S9: The determination of phosphorus species in the liquid phase. References [30,38,61–72] are cited in the Supplementary Materials.

Author Contributions: Conceptualization, K.X.; Formal analysis, B.O., H.W., Y.Z. and Y.L.; Investigation, B.O. and H.W.; Supervision, S.L., H.H., W.Y., J.H. and J.Y.; Writing—original draft, B.O.; Writing—review and editing, K.X. All authors have read and agreed to the published version of the manuscript.

Funding: This study was funded by the National Natural Science Foundation of China (U1901216, 52170133, 51708239).

Data Availability Statement: Not applicable.

Acknowledgments: The work was also supported by the Natural Science Foundation of Hubei Province (No. 2020CFA042), National Key Research and Development Program of China (No. 2019YFC1904003) and Applied Basic Research Program of Wuhan (No. 2020020601012277). The Analytical and Testing Center of Huazhong University of Science and Technology (China) and the Core Facilities of Life Sciences of Huazhong University of Science and Technology (China) are also acknowledged.

Conflicts of Interest: The authors declare that they have no known competing financial interests or personal relationships that could have appeared to influence the work reported in this paper.

References

1. Prasad, S.; Yadav, K.K.; Kumar, S.; Gupta, N.; Cabral-Pinto, M.M.S.; Rezania, S.; Radwan, N.; Alam, J. Chromium contamination and effect on environmental health and its remediation: A sustainable approaches. *J. Environ. Manag.* **2021**, *285*, 112174. [CrossRef] [PubMed]
2. Ukhurebor, K.E.; Aigbe, U.O.; Onyancha, R.B.; Nwankwo, W.; Osibote, O.A.; Paumo, H.K.; Ama, O.M.; Adetunji, C.O.; Siloko, I.U. Effect of hexavalent chromium on the environment and removal techniques: A review. *J. Environ. Manag.* **2021**, *280*, 111809. [CrossRef] [PubMed]
3. Jin, W.; Du, H.; Zheng, S.; Zhang, Y. Electrochemical processes for the environmental remediation of toxic Cr(VI): A review. *Electrochim. Acta* **2016**, *191*, 1044–1055. [CrossRef]
4. Sinha, V.; Pakshirajan, K.; Chaturvedi, R. Chromium tolerance, bioaccumulation and localization in plants: An overview. *J. Environ. Manag.* **2018**, *206*, 715–730. [CrossRef] [PubMed]
5. Haney, J.T.; Erraguntla, N.; Sielken, R.L.; Valdez-Flores, C. Development of an inhalation unit risk factor for hexavalent chromium. *Regul. Toxicol. Pharmacol.* **2014**, *68*, 201–211. [CrossRef]
6. Chen, J.; Tian, Y. Hexavalent chromium reducing bacteria: Mechanism of reduction and characteristics. *Environ. Sci. Pollut. Res.* **2021**, *28*, 20981–20997. [CrossRef]
7. Uddin, M.J.; Jeong, Y.; Lee, W. Microbial fuel cells for bioelectricity generation through reduction of hexavalent chromium in wastewater: A review. *Int. J. Hydrogen. Energ.* **2021**, *46*, 11458–11481. [CrossRef]
8. Veer, S.; Vishal, M. Sustainable reduction of Cr (VI) and its elemental mapping on chitosan coated citrus limetta peels biomass in synthetic wastewater. *Sep. Sci. Technol.* **2022**, *57*, 1609–1626.
9. Jiang, B.; Niu, Q.; Li, C.; Oturan, N.; Oturan, M.A. Outstanding performance of electro-Fenton process for efficient decontamination of Cr(III) complexes via alkaline precipitation with no accumulation of Cr(VI): Important roles of iron species. *Appl. Catal. B Environ.* **2020**, *272*, 119002. [CrossRef]
10. Religa, P.; Kowalik-Klimczak, A.; Gierycz, P. Study on the behavior of nanofiltration membranes using for chromium(III) recovery from salt mixture solution. *Desalination* **2013**, *315*, 115–123. [CrossRef]
11. Sun, P.; Wang, Z.; An, S.; Zhao, J.; Yan, Y.; Zhang, D.; Wu, Z.; Shen, B.; Lyu, H. Biochar-supported nZVI for the removal of Cr(VI) from soil and water: Advances in experimental research and engineering applications. *J. Environ. Manag.* **2022**, *316*, 115211. [CrossRef]
12. Xing, X.; Alharbi, N.S.; Ren, X.; Chen, C. A comprehensive review on emerging natural and tailored materials for chromium contaminated water treatment and environmental remediation. *J. Environ. Chem. Eng.* **2022**, *10*, 107325. [CrossRef]
13. Gopinath, A.; Divyapriya, G.; Srivastava, V.; Laiju, A.R.; Nidheesh, P.V.; Kumar, M.S. Conversion of sewage sludge into biochar: A potential resource in water and wastewater treatment. *Environ. Res.* **2021**, *194*, 110656. [CrossRef]
14. Qiu, Y.; Zhang, Q.; Gao, B.; Li, M.; Fan, Z.; Sang, W.; Hao, H.; Wei, X. Removal mechanisms of Cr(VI) and Cr(III) by biochar supported nanosized zero-valent iron: Synergy of adsorption, reduction and transformation. *Environ. Pollut.* **2020**, *265*, 115018. [CrossRef]

15. Chen, T.; Zhou, Z.; Xu, S.; Wang, H.; Lu, W. Adsorption behavior comparison of trivalent and hexavalent chromium on biochar derived from municipal sludge. *Bioresour. Technol.* **2015**, *190*, 388–394. [CrossRef]
16. Diao, Z.; Du, J.; Jiang, D.; Kong, L.; Huo, W.; Liu, C.; Wu, Q.; Xu, X. Insights into the simultaneous removal of Cr^{6+} and Pb^{2+} by a novel sewage sludge-derived biochar immobilized nanoscale zero valent iron: Coexistence effect and mechanism. *Sci. Total Environ.* **2018**, *642*, 505–515. [CrossRef]
17. Wang, H.; Xiao, K.; Yang, J.; Yu, Z.; Yu, W.; Xu, Q.; Wu, Q.; Liang, S.; Hu, J.; Hou, H.; et al. Phosphorus recovery from the liquid phase of anaerobic digestate using biochar derived from iron-rich sludge: A potential phosphorus fertilizer. *Water Res.* **2020**, *174*, 115629. [CrossRef]
18. Costa, R.C.C.; Moura, F.C.C.; Oliveira, P.E.F.; Magalhães, F.; Ardisson, J.D.; Lago, R.M. Controlled reduction of red mud waste to produce active systems for environmental applications: Heterogeneous Fenton reaction and reduction of Cr(VI). *Chemosphere* **2010**, *78*, 1116–1120. [CrossRef]
19. Wang, X.; Gu, L.; Zhou, P.; Zhu, N.; Li, C.; Tao, H.; Wen, H.; Zhang, D. Pyrolytic temperature dependent conversion of sewage sludge to carbon catalyst and their performance in persulfate degradation of 2-Naphthol. *Chem. Eng. J.* **2017**, *324*, 203–215. [CrossRef]
20. Qin, J.; Li, Q.; Liu, Y.; Niu, A.; Lin, C. Biochar-driven reduction of As(V) and Cr(VI): Effects of pyrolysis temperature and low-molecular-weight organic acids. *Ecotoxicol. Environ. Saf.* **2020**, *201*, 110873. [CrossRef]
21. Hashem, M.A.; Payel, S.; Mim, S.S.; Hasan, M.A.; Nur-A-Tomal, M.S.; Rahman, M.A.; Sarker, M.I. Chromium adsorption on surface activated biochar made from tannery liming sludge: A waste-to-wealth approach. *Water Sci. Eng.* **2022**, *15*, 328–336. [CrossRef]
22. Xu, Z.; Xu, X.; Zhang, Y.; Yu, Y.; Cao, X. Pyrolysis-Temperature depended electron donating and mediating mechanisms of biochar for Cr(VI) reduction. *J. Hazard. Mater.* **2020**, *388*, 121794. [CrossRef] [PubMed]
23. Priester, J.H.; Olson, S.G.; Webb, S.M.; Neu, M.P.; Hersman, L.E.; Holden, P.A. Enhanced exopolymer production and chromium stabilization in *Pseudomonas putida* unsaturated biofilms. *Appl. Environ. Microb.* **2006**, *72*, 1988–1996. [CrossRef]
24. Wani, P.A.; Wani, J.A.; Wahid, S. Recent advances in the mechanism of detoxification of genotoxic and cytotoxic Cr (VI) by microbes. *J. Environ. Chem. Eng.* **2018**, *6*, 3798–3807. [CrossRef]
25. Sathishkumar, K.; Murugan, K.; Benelli, G.; Higuchi, A.; Rajasekar, A. Bioreduction of hexavalent chromium by *Pseudomonas stutzeri* L1 and *Acinetobacter baumannii* L2. *Ann. Microbiol.* **2017**, *67*, 91–98. [CrossRef]
26. Song, H.; Liu, Y.; Xu, W.; Zeng, G.; Aibibu, N.; Xu, L.; Chen, B. Simultaneous Cr(VI) reduction and phenol degradation in pure cultures of *Pseudomonas aeruginosa* CCTCC AB91095. *Bioresour. Technol.* **2009**, *100*, 5079–5084. [CrossRef]
27. Kang, C.; Wu, P.; Li, L.; Yu, L.; Ruan, B.; Gong, B.; Zhu, N. Cr(VI) reduction and Cr(III) immobilization by resting cells of *Pseudomonas aeruginosa* CCTCC AB93066: Spectroscopic, microscopic, and mass balance analysis. *Environ. Sci. Pollut. Res.* **2017**, *24*, 5949–5963. [CrossRef]
28. Ackerley, D.F.; Gonzalez, C.F.; Park, C.H.; Blake, R.; Keyhan, M.; Matin, A. Chromate-reducing properties of soluble flavoproteins from *Pseudomonas putida* and *Escherichia coli*. *Appl. Environ. Microbiol.* **2004**, *70*, 873–882. [CrossRef]
29. Yu, Z.; Sun, M.; Xiao, K.; Ou, B.; Liang, S.; Hou, H.; Yang, J. Changes of phosphorus species during (hydro) thermal treatments of iron-rich sludge and their solubilization mediated by a phosphate solubilizing microorganism. *Sci. Total Environ.* **2022**, *838*, 156612. [CrossRef]
30. Xiao, K.; Yu, Z.; Wang, H.; Yang, J.; Liang, S.; Hu, J.; Hou, H.; Liu, B. Investigation on emission control of NO_x precursors and phosphorus reclamation during pyrolysis of ferric sludge. *Sci. Total Environ.* **2019**, *670*, 932–940. [CrossRef]
31. Qian, T.; Yang, Q.; Jun, D.; Dong, F.; Zhou, Y. Transformation of phosphorus in sewage sludge biochar mediated by a phosphate-solubilizing microorganism. *Chem. Eng. J.* **2019**, *359*, 1573–1580. [CrossRef]
32. Zhang, H.; Lu, H.; Wang, J.; Zhou, J.; Sui, M. Cr(VI) reduction and Cr(III) immobilization by *Acinetobacter* sp. HK-1 with the assistance of a novel quinone/graphene oxide composite. *Environ. Sci. Technol.* **2014**, *48*, 12876–12885. [CrossRef] [PubMed]
33. He, D.; Zheng, M.; Ma, T.; Li, C.; Ni, J. Interaction of Cr(VI) reduction and denitrification by strain *Pseudomonas aeruginosa* PCN-2 under aerobic conditions. *Bioresour. Technol.* **2015**, *185*, 346–352. [CrossRef] [PubMed]
34. Puzon, G.J.; Roberts, A.G.; Kramer, D.M.; Xun, L. Formation of soluble organo-chromium(III) complexes after chromate reduction in the presence of cellular organics. *Environ. Sci. Technol.* **2005**, *39*, 2811–2817. [CrossRef] [PubMed]
35. Rajapaksha, A.U.; Alam, M.S.; Chen, N.; Alessi, D.S.; Igalavithana, A.D.; Tsang, D.C.W.; Ok, Y.S. Removal of hexavalent chromium in aqueous solutions using biochar: Chemical and spectroscopic investigations. *Sci. Total Environ.* **2018**, *625*, 1567–1573. [CrossRef]
36. Zhou, B.; Chen, T. Biodegradation of phenol with chromium (VI) reduction by the *Pseudomonas* sp. strain JF122. *Desalination Water Treat.* **2016**, *57*, 3544–3551. [CrossRef]
37. Li, Y.; Wang, H.; Wu, P.; Yu, L.; Rehman, S.; Wang, J.; Yang, S.; Zhu, N. Bioreduction of hexavalent chromium on goethite in the presence of *Pseudomonas aeruginosa*. *Environ. Pollut.* **2020**, *265*, 114765. [CrossRef]
38. Zhang, B.; Jiao, W. Biochar facilitated bacterial reduction of Cr(VI) by *Shewanella Putrefaciens* CN32: Pathways and surface characteristics. *Environ. Res.* **2022**, *214*, 113971. [CrossRef]
39. Xu, X.; Huang, H.; Zhang, Y.; Xu, Z.; Cao, X. Biochar as both electron donor and electron shuttle for the reduction transformation of Cr(VI) during its sorption. *Environ. Pollut.* **2019**, *244*, 423–430. [CrossRef]
40. Viti, C.; Marchi, E.; Decorosi, F.; Giovannetti, L. Molecular mechanisms of Cr(VI) resistance in bacteria and fungi. *FEMS Microbiol. Rev.* **2014**, *38*, 633–659. [CrossRef]

41. Hale, S.E.; Alling, V.; Martinsen, V.; Mulder, J.; Breedveld, G.D.; Cornelissen, G. The sorption and desorption of phosphate-P, ammonium-N and nitrate-N in cacao shell and corn cob biochars. *Chemosphere* **2013**, *91*, 1612–1619. [CrossRef]
42. Yu, L.; Huang, H.; Wang, X.; Li, S.; Feng, N.; Zhao, H.; Huang, X.; Li, Y.; Li, H.; Cai, Q.; et al. Novel phosphate-solubilising bacteria isolated from sewage sludge and the mechanism of phosphate solubilisation. *Sci. Total Environ.* **2019**, *658*, 474–484. [CrossRef]
43. Acevedo, E.; Galindo-Castañeda, T.; Prada, F.; Navia, M.; Romero, H.M. Phosphate-solubilizing microorganisms associated with the rhizosphere of oil palm (Elaeis guineensis Jacq.) in Colombia. *Appl. Soil Ecol.* **2014**, *80*, 26–33. [CrossRef]
44. Yang, S.; Wen, Q.; Chen, Z. Effect of KH_2PO_4-modified biochar on immobilization of Cr, Cu, Pb, Zn and as during anaerobic digestion of swine manure. *Bioresour. Technol.* **2021**, *339*, 125570. [CrossRef]
45. Liang, J.; Huang, X.; Yan, J.; Li, Y.; Zhao, Z.; Liu, Y.; Ye, J.; Wei, Y. A review of the formation of Cr(VI) via Cr(III) oxidation in soils and groundwater. *Sci. Total Environ.* **2021**, *774*, 145762. [CrossRef]
46. Su, Y.; Yuan, S.; Guo, Y.; Tan, Y.; Mao, H.; Cao, Y.; Chen, Y. Highly efficient and sustainable removal of Cr(VI) in aqueous solutions by photosynthetic bacteria supplemented with phosphor salts. *Chemosphere* **2021**, *283*, 131031. [CrossRef]
47. Adhikari, S.; Gascó, G.; Méndez, A.; Surapaneni, A.; Jegatheesan, V.; Shah, K.; Paz-Ferreiro, J. Influence of pyrolysis parameters on phosphorus fractions of biosolids derived biochar. *Sci. Total Environ.* **2019**, *695*, 133846. [CrossRef]
48. Figueiredo, C.C.d.; Reis, A.d.S.P.J.; Araujo, A.S.d.; Blum, L.E.B.; Shah, K.; Paz-Ferreiro, J. Assessing the potential of sewage sludge-derived biochar as a novel phosphorus fertilizer: Influence of extractant solutions and pyrolysis temperatures. *Waste Manag.* **2021**, *124*, 144–153. [CrossRef]
49. Wang, Z.; Chen, H.; Zhu, Z.; Xing, S.; Wang, S.; Chen, B. Low-Temperature straw biochar: Sustainable approach for sustaining higher survival of *B. megaterium* and managing phosphorus deficiency in the soil. *Sci. Total Environ.* **2022**, *830*, 154790. [CrossRef]
50. Mortazavian, S.; An, H.; Chun, D.; Moon, J. Activated carbon impregnated by zero-valent iron nanoparticles (AC/nZVI) optimized for simultaneous adsorption and reduction of aqueous hexavalent chromium: Material characterizations and kinetic studies. *Chem. Eng. J.* **2018**, *353*, 781–795. [CrossRef]
51. Zhang, S.; Lyu, H.; Tang, J.; Song, B.; Zhen, M.; Liu, X. A novel biochar supported CMC stabilized nano zero-valent iron composite for hexavalent chromium removal from water. *Chemosphere* **2019**, *217*, 686–694. [CrossRef] [PubMed]
52. Pan, J.; Jiang, J.; Xu, R. Removal of Cr(VI) from aqueous solutions by Na_2SO_3/$FeSO_4$ combined with peanut straw biochar. *Chemosphere* **2014**, *101*, 71–76. [CrossRef] [PubMed]
53. Zhang, Q.; Ye, X.; Chen, D.; Xiao, W.; Zhao, S.; Li, J.; Li, H. Chromium(VI) removal from synthetic solution using novel zero-valent iron biochar composites derived from iron-rich sludge via one-pot synthesis. *J. Water Process* **2022**, *47*, 102720. [CrossRef]
54. Zheng, X.; Xu, W.; Dong, J.; Yang, T.; Shangguan, Z.; Qu, J.; Li, X.; Tan, X. The effects of biochar and its applications in the microbial remediation of contaminated soil: A review. *J. Hazard. Mater.* **2022**, *438*, 129557. [CrossRef]
55. Li, Y.; Chen, X.; Liu, L.; Liu, P.; Zhou, Z.; Hu, H.; Wu, Y.; Lei, T. Characteristics and adsorption of Cr(VI) of biochar pyrolyzed from landfill leachate sludge. *J. Anal. Appl. Pyrol.* **2022**, *162*, 105449. [CrossRef]
56. Ai, D.; Tang, Y.; Yang, R.; Meng, Y.; Wei, T.; Wang, B. Hexavalent chromium (Cr(VI)) removal by ball-milled iron-sulfur @biochar based on P-recovery: Enhancement effect and synergy mechanism. *Bioresour. Technol.* **2023**, *371*, 128598. [CrossRef]
57. Wang, M.; Zhao, Z.; Zhang, Y. Magnetite-Contained biochar derived from Fenton sludge modulated electron transfer of microorganisms in anaerobic digestion. *J. Hazard. Mater.* **2021**, *403*, 123972. [CrossRef]
58. Su, C.; Wang, S.; Zhou, Z.; Wang, H.; Xie, X.; Yang, Y.; Feng, Y.; Liu, W.; Liu, P. Chemical processes of Cr(VI) removal by Fe-modified biochar under aerobic and anaerobic conditions and mechanism characterization under aerobic conditions using synchrotron-related techniques. *Sci. Total Environ.* **2021**, *768*, 144604. [CrossRef]
59. Lan, G.; Fan, Q.; Liu, Y.; Chen, C.; Li, G.; Liu, Y.; Yin, X. Rhamnolipid production from waste cooking oil using *Pseudomonas* SWP-4. *Biochem. Eng. J.* **2015**, *101*, 44–54. [CrossRef]
60. Kang, S.; Lee, J.; Kim, K. Biosorption of Cr(III) and Cr(VI) onto the cell surface of *Pseudomonas aeruginosa*. *Biochem. Eng. J.* **2007**, *36*, 54–58. [CrossRef]
61. Yu, W.; Yang, J.; Tao, S.; Shi, Y.; Yu, J.; Lv, Y.; Liang, S.; Xiao, K.; Liu, B.; Hou, H.; et al. A comparatively optimization of dosages of oxidation agents based on volatile solids and dry solids content in dewatering of sewage sludge. *Water Res.* **2017**, *126*, 342–350. [CrossRef]
62. Kim, S.O.; Moon, S.H.; Kim, K.W.; Yun, S.T. Pilot scale study on the ex-situ electrokinetic removal of heavy metals from municipal wastewater sludges. *Water Res.* **2002**, *36*, 4765–4774. [CrossRef]
63. USEPA. Method 7196A: Chromium, Hexavalent (Colorimetric). 1992. Available online: https://www.google.com.hk/search?q=Method+7196A%3A+Chromium%2C+Hexavalent+%28Colorimetric&ei=fNQSZJ20Asyy2roP6eazuA4&ved=0ahUKEwid4oaWheD9AhVMmVYBHWnzDOcQ4dUDCA4&uact=5&oq=Method+7196A%3A+Chromium%2C+Hexavalent+%28Colorimetric&gs_lcp=Cgxnd3Mtd2l6LXNlcnAQAzIKCAAQRxDWBBCwAzIKCAAQRxDWBBCwAzIKCAAQRxDWBBCwAzIKCAAQRxDWBBCwAzIKCAAQRxDWBBCwAzIKCAAQRxDWBBCwA0oECEEYAFAAWABgsQ5oAnABeACAAQCIAQCSAQCYAQDIAQjAAQE&sclient=gws-wiz-serp (accessed on 12 February 2023).
64. Yu, Y.; An, Q.; Zhou, Y.; Deng, S.; Miao, Y.; Zhao, B.; Yang, L. Highly synergistic effects on ammonium removal by the co-system of *Pseudomonas stutzeri* XL-2 and modified walnut shell biochar. *Bioresour. Technol.* **2019**, *280*, 239–246. [CrossRef]
65. Hedley, M.; Stewart, J.; Chauhan, B. Changes in inorganic and organic soil phosphorus fractions induced by cultivation practices and by laboratory incubations. *Soil Sci. Soc. Am. J.* **1982**, *46*, 970–976. [CrossRef]

66. Schnell, S.; Ratering, S.; Jansen, K. Simultaneous determination of iron(III), iron(II), and manganese(II) in environmental samples by ion chromatography. *Environ. Sci. Technol.* **1998**, *32*, 1530–1537. [CrossRef]
67. Xu, H.; Sun, Y.; Li, J.; Li, F.; Guan, X. Aging of zerovalent iron in synthetic groundwater: X-ray photoelectron spectroscopy depth profiling characterization and cepassivation with uniform magnetic field. *Environ. Sci. Technol.* **2016**, *50*, 8214–8222. [CrossRef]
68. Ri, C.; Tang, J.; Liu, F.; Lyu, H.; Li, F. Enhanced microbial reduction of aqueous hexavalent chromium by *Shewanella oneidensis* MR-1 with biochar as electron shuttle. *J. Environ. Sci.* **2022**, *113*, 12–25. [CrossRef]
69. Ma, R.; Yan, X.; Pu, X.; Fu, X. An exploratory study on the aqueous Cr(VI) removal by the sulfate reducing sludge-based biochar. *Sep. Purif. Technol.* **2021**, *276*, 119314. [CrossRef]
70. Zhao, X.; Feng, H.; Jia, P.; An, Q.; Ma, M. Removal of Cr(VI) from aqueous solution by a novel ZnO-sludge biochar composite. *Environ. Sci. Pollut. Res. Int.* **2022**, *29*, 83045–83059. [CrossRef]
71. Chen, X.; Fan, G.; Li, H.; Li, Y.; Zhang, R.; Huang, Y.; Xu, X. Nanoscale zero-valent iron particles supported on sludge-based biochar for the removal of chromium (VI) from aqueous system. *Environ. Sci. Pollut. Res. Int.* **2022**, *29*, 3853–3863. [CrossRef]
72. Fei, Y.; Li, M.; Ye, Z.; Guan, J.; Huang, Z.; Xiao, T.; Zhang, P. The pH-sensitive sorption governed reduction of Cr(VI) by sludge derived biochar and the accelerating effect of organic acids. *J. Hazard. Mater.* **2022**, *423*, 127205. [CrossRef] [PubMed]